2025 IEEE/SICE International Symposium on System Integration (SII)
January 21-24, 2025, Munich, Germany

Non-Negative Tensor Factorization of Infant Spontaneous Movements: A Pilot Study for ASD Risk Evaluation of Newborn Infants

Rikuya Yonei[1], Akira Furui[1], Hirokazu Doi[2], Koji Shimatani[3] Hideaki Hayashi[4], Midori Yamamoto[5], Kenichi Sakurai[6], Chisato Mori[5,7] and Toshio Tsuji[1]

***Abstract*— Early detection of infants with autism spectrum disorder (ASD) can lead to effective developmental support. In clinical practice, early screening of 18-month-old infants is implemented using a parent-completed questionnaire. However, research has suggested that signs of ASD may also appear in movement characteristics during the first few months of age. In this paper, we propose a method to evaluate infant movement from videos based on non-negative tensor factorization (NTF) and apply it to ASD risk assessment in the neonatal period. The proposed method applies NTF to pose data estimated from videos, and decomposes the infant's movements into multiple components while considering the linkage between body parts. In the experiment, we evaluated the effectiveness of the proposed method using 36 low-risk infants and 13 high-risk infants for ASD, with the aim of applying the method to ASD risk assessment. The results showed that the proposed method captured the tendency for infants to perform different movements depending on their risk level. Machine learning analysis revealed that the proposed method identified ASD risk with an accuracy exceeding 70%, which was comparable or superior to the existing video evaluation method based on heuristically designed indicators.**

I. Introduction

Autism spectrum disorder (ASD) is a type of neurodevelopmental disorder characterized by difficulties in social interaction and verbal communication, as well as limited interests and repetitive behaviors [1]. Currently, no definitive cure has been established for ASD, but early detection and developmental behavioral interventions have been shown to improve social interaction and academic performance [2], underscoring the importance of early detection.

*This work was supported by JSPS KAKENHI Grant Number JP23K17321.

[1]R. Yonei, A. Furui and T. Tsuji are with the Graduate School of Advanced Science and Engineering, Hiroshima University, 1-4-1, Kagamiyama, Higashi-Hiroshima, Hiroshima, 739-8527, Japan, rikuyayonei@hiroshima-u.ac.jp.

[2]H. Doi is with Department of Information and Management Systems Engineering, Nagaoka University of Technology, 1603-1, Kamitomioka, Nagaoka, Niigata, 940-2188, Japan

[3]K. Shimatani is with Faculty of Health and Welfare, Prefectural University of Hiroshima, 1-1, Gakuen-machi, Mihara, Hiroshima, 723-0053, Japan

[4]H. Hayashi is with Institute for Datability Science, Osaka University, 2-8, Yamadaoka, Suita, Osaka, 565-0871, Japan

[5]M. Yamamoto and C. Mori are with Department of Sustainable Health Science, Center for Preventive Medical Sciences, Chiba University, 1-33 Yayoi-cho, Inage-ku, Chiba, 263-8522, Japan

[6]K. Sakurai is with Department of Nutrition and Metabolic Medicine, Center for Preventive Medical Sciences, Chiba University, 1-33 Yayoi-cho, Inage-ku, Chiba, 263-8522, Japan

[7]C. Mori is with Department of Bioenvironmental Medicine, Graduate School of Medicine, Chiba University, 1-8-1 Inohana, Chuo-ku, Chiba, 260-8670, Japan

A parent-completed questionnaire called the modified checklist in autism toddlers (M-CHAT) [3] is one of the widely used methods for risk screening of infants at 18 months of age. The M-CHAT consists of 23 questions that assess developmental delays in social and cognitive functions and hypersensitivity to sensory stimuli. This method has been validated in previous studies as an effective screening tool for ASD risk in 18-month-old infants [4], [5]. Studies have also suggested that signs of ASD may appear in movement characteristics during the first few months of age, and attempts have been made to predict future ASD risk based on movement assessment [6], [7]. However, as movement assessment is performed visually by physicians, there is a possibility that judgments may differ depending on the individual physician's subjectivity and variations in observation conditions.

To evaluate without subjectivity, a quantitative and automatic method for evaluating infant movement has been proposed based on a system using videos captured by an RGB camera. Caruso et al., for example, analyzed videos from 10 days to 24 weeks of age, demonstrating the potential for evaluating neurodevelopmental disorders, including ASD, from video recordings at 10 days of age [8]. However, studies predicting ASD risk from infant movements in the first few days of life remain scarce. As one of the few studies in this area, Doi et al. demonstrated the feasibility of evaluating ASD risk in infants screened at 18 months of age by analyzing videos of newborns and using a set of heuristically designed indicators [9]. This method focused on the approximate shape of the infant to extract body parts, resulting in ambiguous calculations in the area of the body part. The temporal linkage of the body parts had not been analyzed at that point. Previous studies have reported that motor asymmetry is reported as one of the characteristics of infants with ASD [10]. Therefore, considering the temporal linkage between body parts, calculated based on clear segmentation criteria, may be useful for ASD risk assessment.

This paper proposes a method for quantitatively evaluating infant movements from videos based on pose estimation and non-negative tensor factorization (NTF) [11], and its application to ASD risk assessment. In the proposed method, skeletal points of infants are estimated from videos of newborns using pose estimation, and a tensor is created by stacking spectrograms of time-series waveforms obtained from representative points of body parts. NTF is then applied to the tensor to decompose the infant's movements into multiple basis components while considering the linkage between

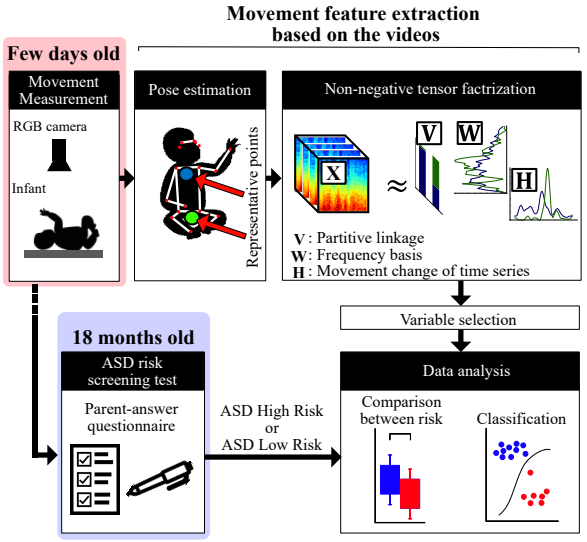

Fig. 1: Overview of the proposed method

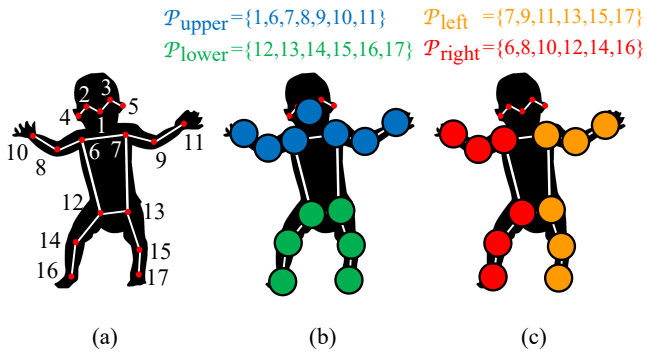

Fig. 2: Pose layout of a single frame. (a) Estimated pose by FiDIP [12]. (b) Skeletal points used to calculate representative points for the upper body (blue points) and lower body (green points). (c) Skeletal points used to calculate representative points for the left side of the body (orange points) and right side of the body (red points).

body parts, thus enabling the extraction of characteristic movement patterns.

II. Methods

An overview of the proposed method is shown in Fig. 1. The proposed method consists of movement measurement using RGB cameras, skeletal point extraction using FiDIP [12], feature extraction using NTF, and data analysis, in that order.

A. Movement Measurement

The infant's movements are measured using a single RGB camera fixed directly above the bed (frame rate: f_{s} [fps], video resolution: $W_{\text{p}} \times H_{\text{p}}$ [pixel]). The infant is placed in a supine position, and the video is recorded so that the whole body remains within the camera's field of view. The segments in which sleep, crying, or external intervention occurs are excluded from the recorded videos. From the remaining segments, we select several continuous segments longer than T_{o} frames.

B. Pose Estimation

A pose estimation model is used to obtain the infant's skeletal points from the extracted video. In this paper, we use fine-tuned domain-adapted infant pose (FiDIP) [12], a model trained on infant videos and generated 3D composite data. By applying FiDIP to the video, 17 skeletal points are estimated for each frame, as shown in Fig. 2(a). The coordinates of the skeletal point estimated at frame l are defined as (u_j^l, v_j^l) $(j \in \{1, 2, \ldots, 17\})$.

We divide the estimated skeletal points into four sets (Fig. 2(b) and (c)): upper body ($\mathcal{P}_{\text{upper}}$), lower body ($\mathcal{P}_{\text{lower}}$), right body ($\mathcal{P}_{\text{right}}$), and left body ($\mathcal{P}_{\text{left}}$), to focus on the linkages among the major body parts. Let $\mathcal{A} = \{\text{upper}, \text{lower}, \text{right}, \text{left}\}$ be the set of body part identifiers. Representative points for each body part $\alpha \in \mathcal{A}$ are then calculated using skeletal points as follows:

$$p_\alpha^l = \frac{1}{|\mathcal{P}_\alpha|} \sqrt{\left(\sum_{j' \in \mathcal{P}_\alpha} u_{j'}^l \right)^2 + \left(\sum_{j' \in \mathcal{P}_\alpha} v_{j'}^l \right)^2}, \quad (1)$$

For example, p_{upper}^l represents the distance from the origin to the average position of the skeletal points belonging to the upper body. This allows us to evaluate the time-series movement changes of the representative points of the upper, lower, left, and right body parts.

To standardize the analysis across infants with varying video lengths, we employ the following procedure to identify segments of significant movement:

1) Calculate the frame-to-frame movement difference p_{diff}^l by summing the changes in representative points across all body parts:
$$p_{\text{diff}}^l = \sum_{\alpha \in \mathcal{A}} \left| p_\alpha^{l+1} - p_\alpha^l \right|. \quad (2)$$
2) Set a threshold p_{th} to identify frames with substantial movement.
3) Apply a sliding window of length T_{o} frames to the video, moving one frame at a time. For each window position, calculate the ratio of frames where $p_{\text{diff}}^l > p_{\text{th}}$.
4) Select for analysis those windows where this ratio exceeds a predetermined percentage p_{per}.

The values of p_{th} and p_{per} are determined empirically to balance sensitivity to movement with the need to exclude minor or incidental motions. This approach allows us to capture multiple instances of significant movement throughout the video. By allowing the selected windows to be non-overlapping, we can identify and analyze all periods of substantial infant movement within a single video, avoiding the limitation of analyzing only a single continuous segment.

C. Feature Extraction Using Non-Negative Tensor Factorization (NTF)

Fig. 3 shows the calculation process flow of movement feature extraction using NTF. To focus on the linkage of the infant's body parts relative to the axis of symmetry, we create two tensors: one for the superior-inferior body axis by stacking the spectrograms of the upper and lower body, and the other for the medial-lateral body axis by stacking the spectrograms of the left and right sides of the body. By applying NTF to these tensors, we extract the frequency basis components of the infant's movements, the time-series movement changes of the angular frequency basis, and the linkage between the movements of each body part.

First, we calculate a moving average for the waveform P_α^l at each representative point of the segment to be analyzed using a window width of τ_{roll} frames. We then remove the offset component by subtracting it from the original waveform. Furthermore, we apply a fourth-order Butterworth low-pass filter (cutoff frequency: f_{cut} [Hz]) to remove high-frequency components unrelated to movement.

Next, we apply a short-time Fourier transform with window width τ_{stft} frames and shift width o_{stft} frames to the preprocessed p_α^l to create a spectrogram $\mathbf{X}^\alpha \in \mathbb{R}^{D\times T}$ (T is the number of elements in the time component; D is the number of elements in the frequency component). We then create two third-order tensors: $\mathbf{X}^{\mathrm{SI}} \in \mathbb{R}^{2\times D\times T}$ for the upper and lower body elements, and $\mathbf{X}^{\mathrm{ML}} \in \mathbb{R}^{2\times D\times T}$ for the right and left body elements. $\mathbf{X}^{\mathrm{SI}}$ is constructed by stacking the spectrograms of the upper body representative point waveform $\mathbf{X}^{\mathrm{upper}}$ and the lower body representative point waveform $\mathbf{X}^{\mathrm{lower}}$ along the first dimension:

$$x^{\mathrm{SI}}_{k,d,t} = \begin{cases} x^{\mathrm{upper}}_{d,t} & \text{for } k=1, \\ x^{\mathrm{lower}}_{d,t} & \text{for } k=2, \end{cases} \tag{3}$$

where $x^\alpha_{d,t}$ denotes the elements of $\mathbf{X}^\alpha$ in d rows and t columns, and $x^{\mathrm{SI}}_{k,d,t}$ denotes the elements of $\mathbf{X}^{\mathrm{SI}}$. Similarly, $\mathbf{X}^{\mathrm{ML}}$ is constructed by stacking the spectrograms of the left body representative point waveform $\mathbf{X}^{\mathrm{left}}$ and the right body representative point waveform $\mathbf{X}^{\mathrm{right}}$ along the first dimension:

$$x^{\mathrm{ML}}_{k,d,t} = \begin{cases} x^{\mathrm{left}}_{d,t} & \text{for } k=1, \\ x^{\mathrm{right}}_{d,t} & \text{for } k=2, \end{cases} \tag{4}$$

where $x^{\mathrm{ML}}_{k,d,t}$ denotes the elements of $\mathbf{X}^{\mathrm{ML}}$.

In this paper, we use NTF to extract representative frequency bands of infant movements from each tensor $\mathbf{X}^i$ ($i \in \{\mathrm{SI}, \mathrm{ML}\}$). The proposed method uses the CANDECOMP/PARAFAC decomposition [11], which decomposes the observed data tensor $\mathbf{X}^i$ into three-factor matrices: $\mathbf{V}^i = [\mathbf{v}^i_1, \ldots, \mathbf{v}^i_M] \in \mathbb{R}^{2\times M}$ (M is the number of basis vectors), $\mathbf{W}^i = [\mathbf{w}^i_1, \ldots, \mathbf{w}^i_M] \in \mathbb{R}^{D\times M}$, and $\mathbf{H}^i = [\mathbf{h}^i_1, \ldots, \mathbf{h}^i_M] \in \mathbb{R}^{T\times M}$. The decomposition can be expressed as:

$$\mathbf{X}^i \approx \sum_{m=1}^{M} \mathbf{v}^i_m \otimes \mathbf{w}^i_m \otimes \mathbf{h}^i_m, \tag{5}$$

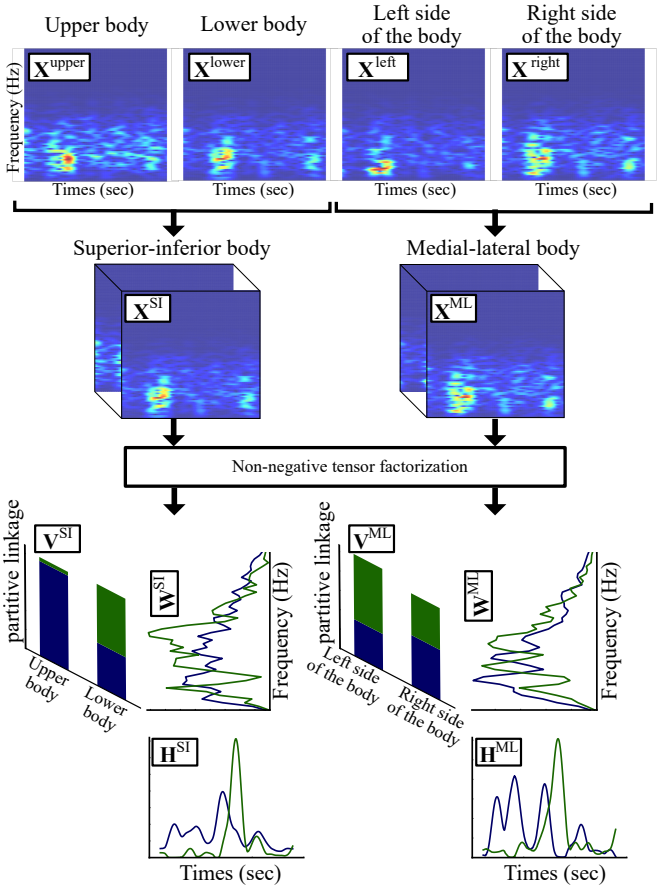

Fig. 3: Process flow of NTF-based movement feature extraction

where $\otimes$ represents the Kronecker product between vectors. The matrix $\mathbf{W}^i$ represents the frequency basis components of the infant's movements, $\mathbf{H}^i$ represents the time-series movement changes of each frequency basis, and $\mathbf{V}^i$ represents the linkages between the movements of each body part at the frequency and time extracted by $\mathbf{W}^i$ and $\mathbf{H}^i$. Therefore, NTF can be used to extract representative frequency bands and time-series movement features for each frequency basis component while considering the linkage between body parts.

III. Experiments

We conducted a movement assessment experiment to evaluate the effectiveness of the proposed method for ASD risk assessment. This experiment was conducted after obtaining approval from the institutional ethical committees of Hiroshima University (Approval No. E-1150-2) and Chiba University (Approval No. 451). Written informed consent was obtained from all nurturer parents of infants.

A. Participants

This experiment was conducted with 49 infants. The analyzed videos were recorded during the newborn period (2.061 ± 0.586 days after birth) at a hospital as part of a long-term health study [13]. The risk of ASD for each infant

was assessed based on the results of the Japanese version of the M-CHAT [3], which was administered at 18 months of age. Infants were classified as high-risk if they were judged atypical in three or more of the 23 question items or in one or more of the 10 critical items; otherwise, they were classified as low-risk. As a result, the 49 infants were categorized into 13 in the high-risk group and 36 in the low-risk group.

B. Implementation Details

This experiment was conducted with a frame rate $f_{\mathrm{s}} = 30$ fps and a resolution of $W_{\mathrm{p}} \times H_{\mathrm{p}} = 1280 \times 720$ pixels. The thresholds for analysis were set to $p_{\mathrm{th}} = 0.3$ and $p_{\mathrm{per}} = 0.85$, respectively, and the length of the analysis segment was set to $T_{\mathrm{o}} = 1800$ frames. As a result, the analysis segments consisted of 40 high-risk infants and 81 low-risk infants. The window width of the moving average was set to $\tau_{\mathrm{roll}} = 15$ frames, the cutoff frequency of the low-pass filter was set to $f_{\mathrm{cut}} = 5$ Hz, and the window and shift width of the STFT were set to $\tau_{\mathrm{stft}} = 256$ frame and $o_{\mathrm{stft}} = 1$ frame. Since NTF results are affected by the initial values, in this experiment, NTF was performed five times with different random numbers, and the result with the highest variance accounted for (VAF) [14], which indicates the degree to which the original tensor was recovered, was used. For the basis number M, which indicates the number of elemental decompositions of the NTF, we calculated the VAF for each infant and used $M = 2$, which is the smallest number whose median value exceeded 0.85.

C. Indicators Calculation for Each Factor Matrix

In the experiment, each factor matrix $\mathbf{W}^i, \mathbf{H}^i, \mathbf{V}^i$ obtained by NTF analysis was used to define an indicator to evaluate the differences between low-risk and high-risk infants.

For the factor matrices $\mathbf{W}^i$ and $\mathbf{H}^i$, a total of four indicators were calculated for each basis component ($m = 1, \ldots, M$) and tensor ($i \in \{\mathrm{SI}, \mathrm{ML}\}$) as described below. In addition, for the factor matrix $\mathbf{V}^i$, we first obtained the amplitude values scaled by the MinMax method for each infant and tensor ($i \in \{\mathrm{SI}, \mathrm{ML}\}$). Then, these obtained amplitude values were used as indicators for each basis component ($m = 1, \ldots, M$) and each body part ($\alpha \in \mathcal{A}$).

- $w^i_{\mathrm{peak},m}$: Peak frequency of matrix $\mathbf{W}^i$.
- $w^i_{\mathrm{mid},m}$: Center frequency of matrix $\mathbf{W}^i$.
- $h^i_{\mathrm{ave},m}$: Amplitude average of matrix $\mathbf{H}^i$.
- $h^i_{\mathrm{std},m}$: Amplitude standard deviation of matrix $\mathbf{H}^i$.
- $v^i_{\alpha,m}$: Scaled amplitude values of matrix $\mathbf{V}^i$.

To unify the interpretation of the analysis results, the frequency vectors after NTF were sorted in ascending order of their peak frequencies. In cases where peak frequencies were equal, the vectors were sorted by center frequency.

D. Variable Selection and ASD Risk Group Classification

Variable selection was performed to extract useful indicators for ASD risk assessment from the calculated indicator groups. The Boruta method [15] was used as the variable selection method. This method compares the variable importance of the shadow variable, which does not correlate with the objective variable, to the variable importance of the explanatory variable, and selects explanatory variables that contribute more to the objective variable than the shadow variable. In this experiment, variable importance was calculated using a random forest. Because random forest results are affected by random numbers, the Boruta method was applied with different random numbers seven times, and the indicator values selected four or more times were evaluated. Cliff's delta [16], a type of effect size, was used to quantify the difference in indicator values between groups.

Classification experiments were conducted using a random forest to verify the usefulness of the selected indicator groups for ASD risk assessment. Classifier performance was evaluated based on nested-stratified-4-fold cross-validation (nested-CV), with hyperparameter tuning performed simultaneously. Nested-CV was performed seven times with different random numbers to reduce their influence. The classification results for each fold were then combined using a majority vote ensemble. The risk of ASD for each infant was defined as high risk if more than half of the segments were classified as having a high risk of ASD, and low otherwise.

For comparison with the proposed method, the indicators calculated by the Doi et al. method [17] were used, and classification was performed under the same settings as the proposed method. The performance measures used were accuracy, recall, specificity, and Matthews correlation coefficient (MCC) [18].

IV. Results

Fig. 4 shows the relationship between the waveforms of each factor matrix after NTF and the corresponding video. Dark blue represents the first basis component and green represents the second basis component. In Fig. 4(a), movements of the upper limb are accompanied by no movements of the lower limb in the dominant segment of the second basis. In Fig. 4(b), a reflex-like movement of the hand was observed in the dominant segment of the second basis.

Fig. 5 shows the results of variable selection. Blue represents low-risk infants and red represents high-risk infants. The figure shows that high-risk infants tended to have a weak lower body linkage and high peak frequency in the second basis of the tensor $\mathbf{X}^{\mathrm{SI}}$, which has elements of the upper and lower body, while, the tensor $\mathbf{X}^{\mathrm{ML}}$ with elements of the left and right sides of the body showed a smaller standard deviation in the time-series movement changes of the second basis. All effect sizes were small.

Fig. 6 and Table I show the results of the classification experiment. The maximum value of each evaluation metric is shown in bold. The figure and table show that the proposed method tends to improve the recall compared to the conventional method, while maintaining the same specificity.

V. Discussion

As a result of variable selection, three indicators were selected (Fig. 5). High-risk infants tended to have weaker lower body linkage in the second basis of the superior-inferior body axis tensor $\mathbf{X}^{\mathrm{SI}}$ ($v^{\mathrm{SI}}_{\mathrm{lower},2}$). Previous studies have reported

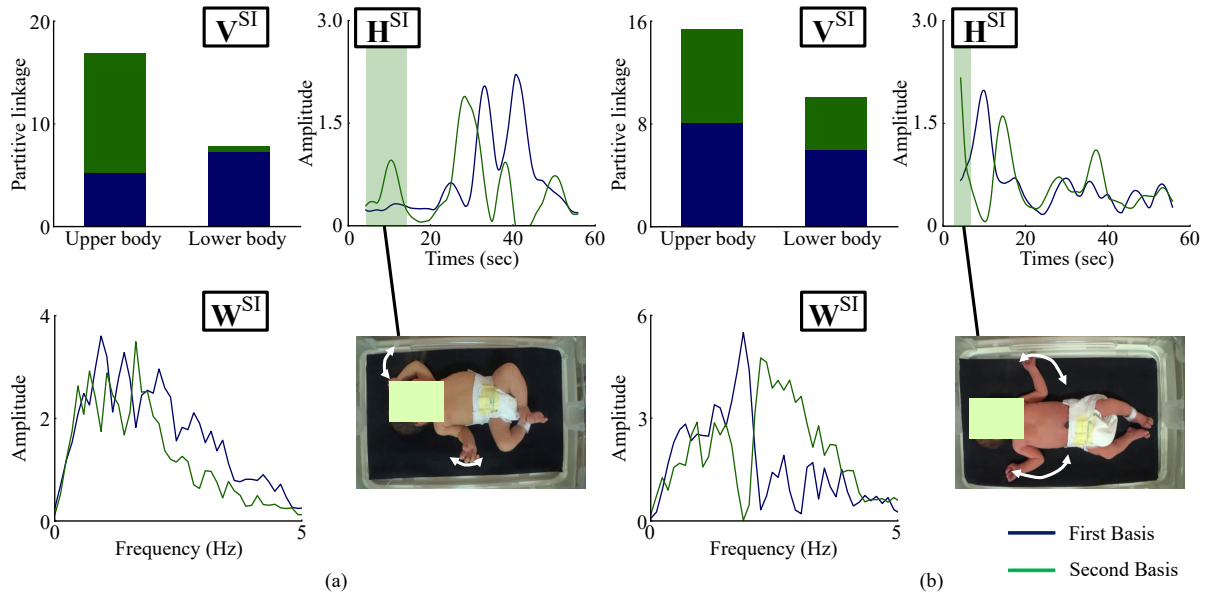

Fig. 4: Example of NTF results and corresponding infant's video. (a) Results of Sub. A (high-risk infant). (b) Results of Sub. B (high-risk infant).

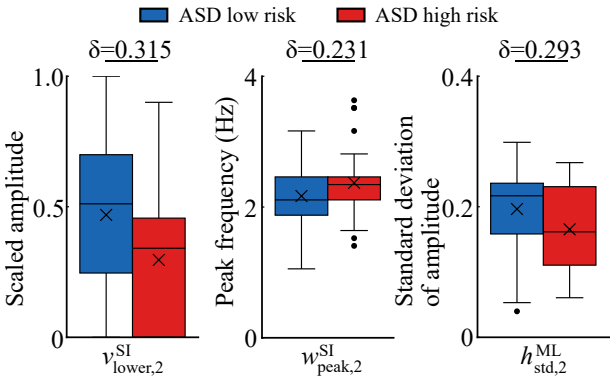

Fig. 5: Experimental results of selected indicators. Effect size metrics using Cliff's delta are also shown.

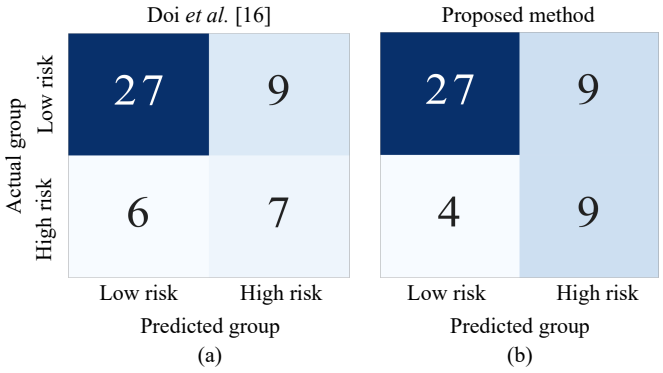

Fig. 6: Confusion matrix for each method

TABLE I: Evaluation metrics for each method

Method	Accuracy	Recall	Specificity	MCC
Doi *et al.* [17]	0.694	0.538	**0.750**	0.272
Proposed method	**0.735**	**0.692**	**0.750**	**0.405**

developmental delay in lower limb movements in infants with ASD, such as passive lower limb movements during walking [19]. Correspondence between the NTF results and video observations showed that high-risk infants with weak lower body coordination in the second basis exhibited significant upper limb movements while their lower limbs remained stationary when the second basis was dominant (Fig. 4(a)). Thus, high-risk infants performed more arm-only movements than low-risk infants, possibly reflecting delayed motor development of the lower body. Since it has been suggested that signs of motor developmental delay in the lower body appear around four months of age [17], the results of this experiment suggest the possibility of earlier assessment of motor development in infants. Therefore, an NTF-based movement assessment method that considers body part linkage over time may be useful for detecting movement asymmetry in the symmetry axis, a characteristic feature of ASD.

The frequency bands in the second basis of $\mathbf{X}^{\mathrm{SI}}$ ($w^{\mathrm{SI}}_{\mathrm{peak},2}$) tended to be high. Correspondence between the NTF results and videos showed several spasmodic movements, such as momentary large movements of the hands, where both hands were momentarily spread wide as if startled, in segments where the second basis was dominant for high-risk infants with a high-frequency band in the second basis (Fig. 4(b)). Previous studies have reported that infants with abnormalities in general movements (GMs) are at higher risk for ASD [20], and lack of smoothness and monotonicity of movements are known to be abnormal GMs from birth to nine weeks of age [21]. Thus, spasmodic movements in high-risk infants may be due to a lack of smooth movement. The standard

deviations in the time-series movement changes of the second basis of $\mathbf{X}^{\mathrm{ML}}$ ($h^{\mathrm{ML}}_{\mathrm{std},2}$) tended to be small. High-risk infants with these characteristics tended to have smaller peaks of time-series movement changes. This result may reflect signs of motor development specific to infants at risk for ASD, indicating the need for a new indicator of time-series movement changes for more detailed analysis.

Results of the classification experiment showed that the proposed method improved all evaluation measures except specificity, which remained unchanged compared to the conventional method. The results indicate that the proposed method can identify ASD risk with the same or better performance than the conventional method without using heuristically designed indicators. As mentioned earlier, movement asymmetry along the axis of symmetry has been reported as a characteristic of infants with ASD. The proposed method can consider the linkage between body parts in a time-series pattern, which may slightly reduce false classifications compared to the conventional method.

VI. Conclusions

In this paper, we proposed a method for evaluating infant movements from videos using pose estimation and NTF and applied it to the evaluation of ASD risk. In the proposed method, representative points in each body part of an infant are calculated from skeletal points obtained by applying pose estimation to videos, and a tensor created from the spectrogram of the time-series waveforms of the representative points is decomposed by NTF. This method enables the extraction of movements that take into account the linkage between the body parts of the infant.

In the experiment, the proposed method was applied to videos of newborn infants (2.061 ± 0.586 days), and their relationship with ASD risk at 18 months of age were analyzed (low-risk infants: 36, high-risk infants: 13). As a result, we confirmed that infants at high risk for ASD performed movements differently from those at low risk, and demonstrated that this characteristic may be related to previously reported signs of ASD risk. Furthermore, we confirmed that the proposed method can identify ASD risk with the same or better performance than conventional methods, without relying on heuristic indicator design.

However, as only 49 infants were included in the analysis in this paper, it is not possible to determine the true usefulness of the proposed method or its generalization performance for ASD risk classification. Further study should increase the number of participants.

References

[1] American Psychiatric Association, *Diagnostic and Statistical Manual of Mental Disorders, Fifth Edition (DSM-5)*. American Psychiatric Association Publishing, 2013.

[2] G. Cioni, E. Inguaggiato, and G. Sgandurra, "Early intervention in neurodevelopmental disorders: underlying neural mechanisms," *Developmental Medicine & Child Neurology*, vol. 58, pp. 61–66, 2016.

[3] D. L. Robins, D. Fein, M. L. Barton, and J. A. Green, "The Modified Checklist for Autism in Toddlers: an initial study investigating the early detection of autism and pervasive developmental disorders," *Journal of Autism and Developmental Disorders*, vol. 31, no. 2, pp. 131–144, 2001.

[4] F. Thabtah and D. Peebles, "Early autism screening: a comprehensive review," *International Journal of Environmental Research and Public Health*, vol. 16, no. 18, p. 3502, 2019.

[5] N. Inada, T. Koyama, E. Inokuchi, M. Kuroda, and Y. Kamio, "Reliability and validity of the Japanese version of the Modified Checklist for autism in toddlers (M-CHAT)," *Research in Autism Spectrum Disorders*, vol. 5, no. 1, pp. 330–336, 2011.

[6] K. Libertus, K. A. Sheperd, S. W. Ross, and R. J. Landa, "Limited fine motor and grasping skills in 6-month-old infants at high risk for autism," *Child Development*, vol. 85, no. 6, pp. 2218–2231, 2014.

[7] E. S. LeBarton and R. J. Landa, "Infant motor skill predicts later expressive language and autism spectrum disorder diagnosis," *Infant Behavior and Development*, vol. 54, pp. 37–47, 2019.

[8] C. Angela, M. O. Ribas, M. Micai, M. Bernava, G. Tartarisco, D. L. Pérez, M. Fazio, P. Tomalski, and M. L. Scattoni, "Using DeepLabCut to recognize early motor development patterns associated with Neurodevelopmental Disorders," *IEEE Access*, 2024.

[9] H. Doi, A. Furui, R. Ueda, K. Shimatani, M. Yamamoto, K. Sakurai, C. Mori, and T. Tsuji, "Spatiotemporal patterns of spontaneous movement in neonates are significantly linked to risk of autism spectrum disorders at 18 months old," *Scientific Reports*, vol. 13, no. 1, p. 13869, 2023.

[10] G. Esposito, P. Venuti, S. Maestro, and F. Muratori, "An exploration of symmetry in early autism spectrum disorders: analysis of lying," *Brain and Development*, vol. 31, no. 2, pp. 131–138, 2009.

[11] T. G. Kolda and B. W. Bader, "Tensor decompositions and applications," *SIAM review*, vol. 51, no. 3, pp. 455–500, 2009.

[12] X. Huang, N. Fu, S. Liu, and S. Ostadabbas, "Invariant representation learning for infant pose estimation with small data," in *Proceedings of the 16th IEEE International Conference on Automatic Face and Gesture Recognition (FG 2021)*, 2021, pp. 1–8.

[13] K. Sakurai, H. Miyaso, A. Eguchi, Y. Matsuno, M. Yamamoto, E. Todaka, H. Fukuoka, A. Hata, and C. Mori, "Chiba study of Mother and Children's Health (C-MACH): Cohort study with omics analyses," *BMJ Open*, vol. 6, no. 1, p. e010531, 2016.

[14] G. Torres-Oviedo, J. M. Macpherson, and L. H. Ting, "Muscle synergy organization is robust across a variety of postural perturbations," *Journal of Neurophysiology*, vol. 96, no. 3, pp. 1530–1546, 2006.

[15] M. B. Kursa and W. R. Rudnicki, "Feature selection with the Boruta package," *Journal of Statistical Software*, vol. 36, pp. 1–13, 2010.

[16] N. Cliff, "Dominance statistics: Ordinal analyses to answer ordinal questions," *Psychological Bulletin*, vol. 114, no. 3, p. 494, 1993.

[17] H. Doi, N. Iijima, A. Furui, Z. Soh, R. Yonei, K. Shinohara, M. Iriguchi, K. Shimatani, and T. Tsuji, "Prediction of autistic tendencies at 18 months of age via markerless video analysis of spontaneous body movements in 4-month-old infants," *Scientific Reports*, vol. 12, no. 1, p. 18045, 2022.

[18] B. W. Matthews, "Comparison of the predicted and observed secondary structure of t4 phage lysozyme," *Biochimica et Biophysica Acta (BBA)-Protein Structure*, vol. 405, no. 2, pp. 442–451, 1975.

[19] P. Teitelbaum, O. Teitelbaum, J. Nye, J. Fryman, and R. G. Maurer, "Movement analysis in infancy may be useful for early diagnosis of autism," *Proceedings of the National Academy of Sciences*, vol. 95, no. 23, pp. 13 982–13 987, 1998.

[20] C. Einspieler, J. Sigafoos, K. D. Bartl-Pokorny, R. Landa, P. B. Marschik, and S. Bölte, "Highlighting the first 5 months of life: general movements in infants later diagnosed with autism spectrum disorder or Rett syndrome," *Research in Autism Spectrum Disorders*, vol. 8, no. 3, pp. 286–291, 2014.

[21] H. F. Prechtl, C. Einspieler, G. Cioni, A. F. Bos, F. Ferrari, and D. Sontheimer, "An early marker for neurological deficits after perinatal brain lesions," *The Lancet*, vol. 349, no. 9062, pp. 1361–1363, 1997.